

Design of a Monopole Antenna for WiFi-UWB Based on Characteristic Mode Theory

Zhong-Gen Wang¹, Rui You^{1,*}, Ming Yang², Jinzhi Zhou³, and Mingqing Wang¹

¹School of Electrical and Information Engineering, Anhui University of Science and Technology, Huainan 232001, China

²School of Electrical and Communications Engineering, West Anhui University, Luan 237012, China

³School Electrical and Information Engineering, Bozhou University, Bozhou 236800, China

ABSTRACT: In this paper, a WiFi-UWB multiband monopole antenna is designed, fabricated, and tested based on the characteristic mode theory, which mainly consists of an L-shaped metal, an “ok”-shaped metal radiator, and a T-shaped metal patch. The substrate dimensions are $40 \times 43 \times 1.6 \text{ mm}^3$, featuring a rectangular ground plate at the substrate’s bottom. The “ok”-shaped metal on the upper surface is composed of a metal ring and a curved finger-shaped metal. To improve impedance matching and broaden the bandwidth, strategic modifications are implemented. Specifically, a rectangular slot is introduced at the top of the L-shaped metal, and the T-shaped metal is rotated 90° counterclockwise and positioned beneath the “ok”-shaped metal. The microstrip feed line, constructed from metal, incorporates a feed point. Simulation results indicate that the antenna effectively covers the frequency ranges of 2.30–2.50 GHz and 3.65–9.77 GHz. At the resonance point, the maximum return loss is below -40 dB , signifying superior directional radiation characteristics. The antenna design is characterized by a wide frequency band, simple structure, and holds significant practical value for multi-frequency communication.

1. INTRODUCTION

Since the invention of the antenna by the Russian scientist Popov in 1894, the antenna has a history of 130 years. From the initial monopole antenna to the later microstrip antenna, antenna is constantly developing. However, traditional antenna has the disadvantages of large volume, single and narrow frequency band, low efficiency, and low intelligence, so it is necessary to propose new technologies to improve these disadvantages. Ultra-Wideband (UWB) technology uses nanosecond non-sine-wave narrow pulse to transmit data, which has high data transmission rate, so it can be used in antenna design and manufacture. UWB antenna has a wide bandwidth coverage, suitable for signal transmission of different frequencies, and small size and high efficiency, so it has been widely used [1–11]. A dual-mode UWB antenna is proposed in [5], which consists of monopole and dipole of the same structure and is excited by a coplanar waveguide. It covers the frequency bands 2.8–20 GHz and 4.4–17.6 GHz, and the isolation degree is 15 dB, which is suitable for UWB communication systems. In [8], a compact UWB unipolar antenna is proposed, which is easy to control return loss. The antenna is cactus-shaped, and the substrate material is liquid crystal polymer. There are three radiation short wires connected on a semicircular ring, which is used to adjust the radiation mechanism of the antenna, and the frequency band covers 2.85–11.85 GHz. The parameters controlling return loss have little influence on the antenna radiation, which makes the antenna have good omnidirectional characteristics. Ref. [11] proposes a compact 4-unit multiple-input multiple-output (MIMO) antenna with a size of

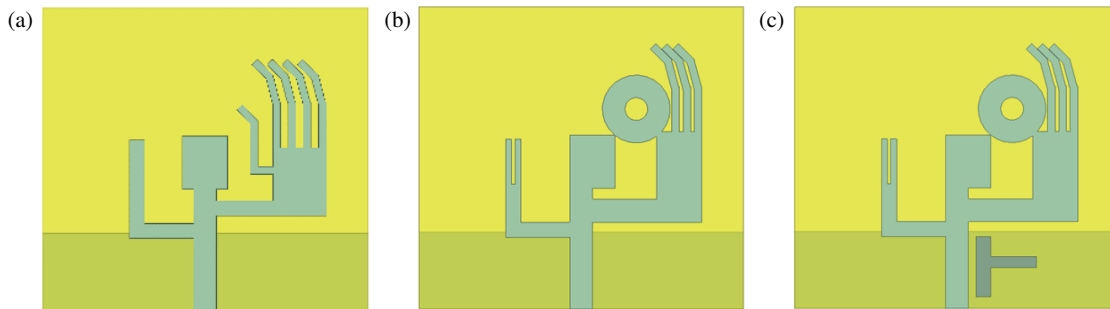
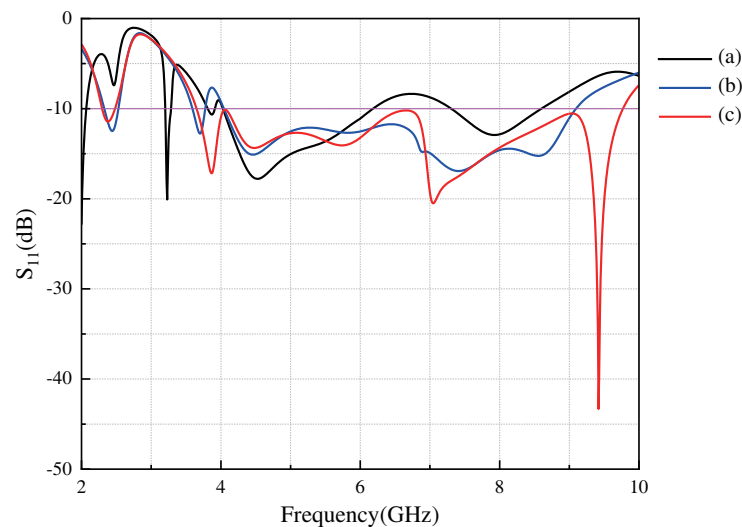
$42 \times 25 \times 1.6 \text{ mm}^3$. Each antenna unit adopts a microstrip fed stepper slot antenna. Due to its own directional radiation characteristics and asymmetric placement, high isolation can be achieved without adding any decoupling network between antenna units. The antenna covers a frequency of 3.1–12 GHz, enabling UWB applications.

The antennas proposed in the above references cover part of the frequency band. The single frequency band of the antenna has a great impact on the high-speed transmission and low delay of the wireless communication network. At the same time now multi-frequency communication is developing rapidly, and more and more devices are supporting multi-frequency communication, so it is a key problem to realize the multi-frequency coverage of the antenna [12–14]. Ref. [12] proposes a conformal multi-frequency antenna for flexible devices, which has a truncated monopole, helpful for realizing multi-frequency bands of 2.45, 3.5, and 5.8 GHz. Simulation results show that the frequency bands that can be covered by this antenna are 2.37–2.5 GHz, 3.37–3.65 GHz, and 5.2–7.7 GHz. The center return loss approaches -40 dB . At first, choosing a popular frequency band is greatly important. Most of the current devices support WiFi connection, and WiFi technology also has many advantages, such as wide coverage, no wiring, and fast transmission speed. At the same time, wireless standard IEEE 802.11a can reach 54 Mbps, which is used in wireless communication, so many antennas are designed to cover the WiFi band [15–18]. In addition, different communication modes use different frequencies, which requires the research of some kinds of antennas containing a variety of frequency bands to meet the use of mainstream WiFi-UWB and other frequency bands [19–23]. Ref. [19] proposes a new com-

* Corresponding author: Rui You (15905597288@139.com).

TABLE 1. Antenna dimensions (mm).

L	W	h	x_1	x_2	x_3	GNDX
40	43	1.6	1.5	0.5	3	10.2
R_1	R_2	CX	CX_1	CX_2	CX_3	CY
4.5	1.5	18.5	8	13	1.5	2.5
CY_1	CY_2	CY_3	xx	xx ₁	yy	yy ₁
2	3.5	7	6	1	0.2	10

**FIGURE 2.** Schematic diagram of antenna structure evolution: (a) Initial structure. (b) Improved structure. (c) Final structure.**FIGURE 3.** S -parameter curves corresponding to (a), (b) and (c) in Figure 2.

$40 \times 43 \times 1.6 \text{ mm}^3$, and the antenna's parameters are shown in Table 1. The length and width of the left L-shaped metal is 13 mm and 9 mm, respectively, and the slot opened above has a width of xx and a length of yy . The length and width of the middle metal trunk are 23 mm and 3 mm, respectively. The head is equal to the hand of the metal of the "ok" gesture on the right side, and both are 6 mm. The finger part of the metal of the "ok" gesture consists of three sections of the metal, and the widths of all of them are 1 mm. The lengths of the three sections of the right hand gesture metal from the top to the bottom are 3 mm, 4 mm and 6 mm, in which the metal on top and the metal in the middle are rotated at an angle. The metal on top is rotated at an angle of 45° , and the metal in the middle is rotated at an angle of 15° . The "o" in "ok" consists of a circle with radius

R_1 minus a concentric circle with radius R_2 , and the length of the backbone is 14.5 mm, where the "T" shaped metal on the lower right is used to improve impedance matching, with dimensions CX_1 , CY_1 , CX_3 , CY_3 , and the backside is designed as a rectangular floor structure, with a length of GNDX (ground floor in the antenna model) and a width the same as that of the substrate.

2.2. Antenna Evolution and Analysis

The evolution of the antenna structure is shown in Figure 2, and the corresponding simulated S -parameter curve is shown in Figure 3. Figure 2(a) shows the initial structure of the antenna. The radiation performance of each mode can be analyzed by ob-

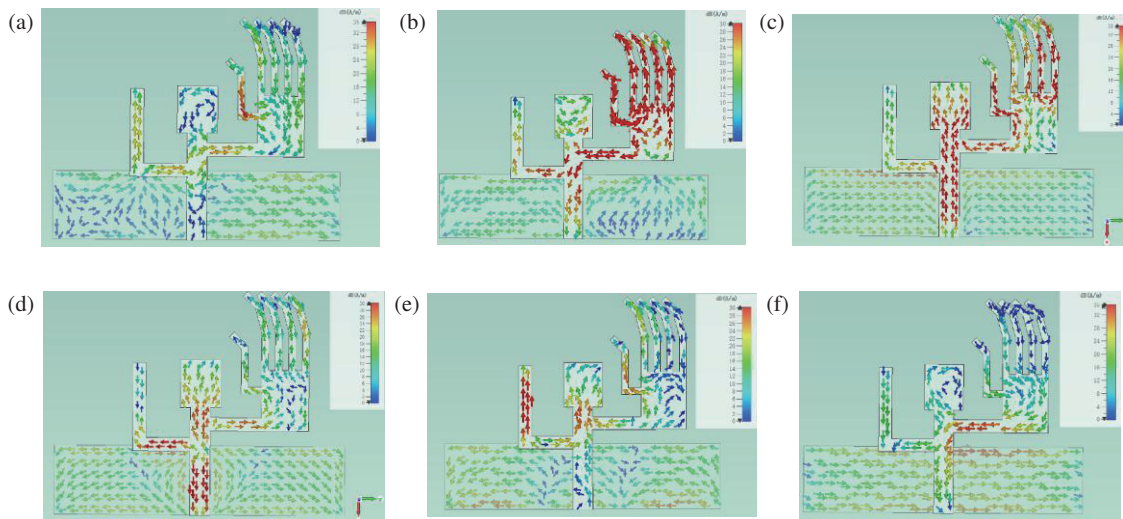


FIGURE 4. Mode current distribution of the initial structure: (a) mode 2 at 6.5 GHz (b) mode 3 at 3.98 GHz (c) mode 5 at 3.37 GHz (d) mode 6 at 8.3 GHz (e) mode 8 at 8.8 GHz (f) mode 9 at 2.45 GHz.

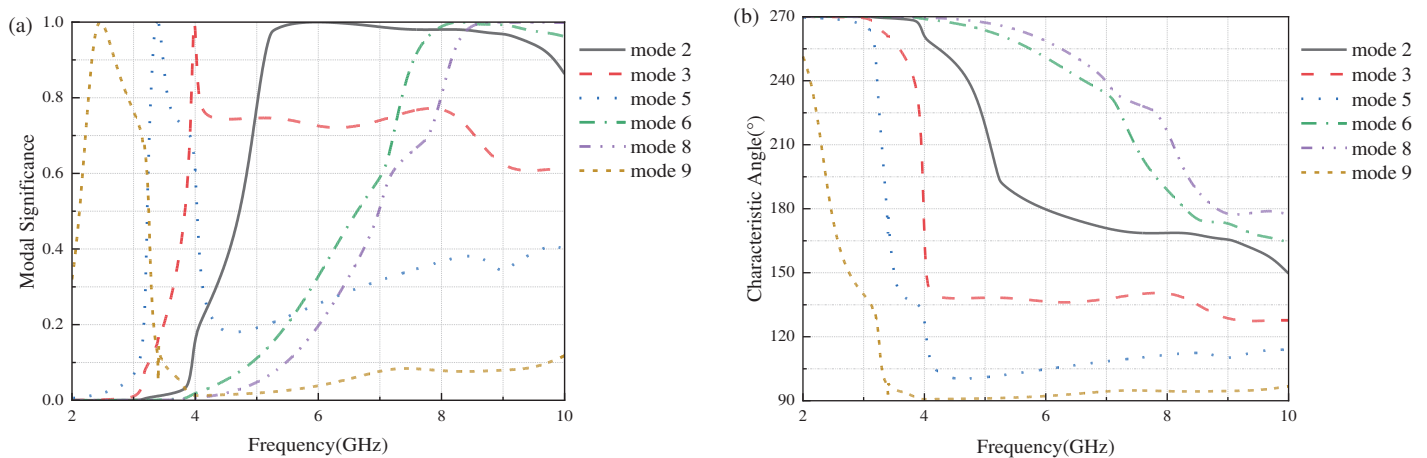


FIGURE 5. The results of mode analysis of the initial structure: (a) MS (b) CA.

serving the Modal Significance (MS) and Characteristic Angle (CA) curves of the antenna. The resonant point current distribution of its characteristic mode under CST software is shown in Figure 4.

It can be seen from the S -parameter curve corresponding to Figure 3(a) that the antenna covers 3.20–3.28 GHz, 4.03–6.18 GHz, and 7.30–8.60 GHz, which does not meet the requirements of UWB antennas. Therefore, the structure of the antenna should be improved.

It can be seen from Figure 4 that the current distribution of mode 3, mode 5, and mode 6 in the feed port is relatively dense, indicating that the current is strong here, where the current of mode 5 flows in the negative direction along the x axis; the currents of mode 3 and mode 6 move along the x axis towards the feed port; and the currents of mode 2, mode 8, and mode 9 have weak current distribution near their feed ports, indicating that these modes are difficult to excite. The radiation performance of each mode can be analyzed by observing the MS and CA curves of the antenna.

The MS value represents the proportion of resonance generated by each mode in a specific frequency range. The closer the MS value is to 1, the more likely the mode is to resonate and to be excited by a suitable feedline, and the less likely the mode is to resonate if the MS value is lower than 0.707. The CA expresses the antenna's resonance performance, and the closer the value of CA is to 180° , the more likely the mode is to resonate. The MS and CA of the initial structure are shown in Figure 5, from which it can be seen that mode 3, mode 5, and mode 6 resonate at 3.98 GHz, 3.37 GHz, and 8.3 GHz, respectively, and the MS of mode 6 is always greater than 0.9 in the frequency band of $f > 7.6$ GHz. The value of CA is also located near 180° . In order for mode 2 and mode 8 to be excited and to enhance the current of mode 9 at the top of the metal backbone and at the hand, the antenna structure is improved, and the improved structure is shown in Figure 2(b).

Bring the thumb and forefinger of the right hand “gesture” metal together to form a circle, so that the entire right hand “fingers” form an “ok” shape, and connect the head of the metal

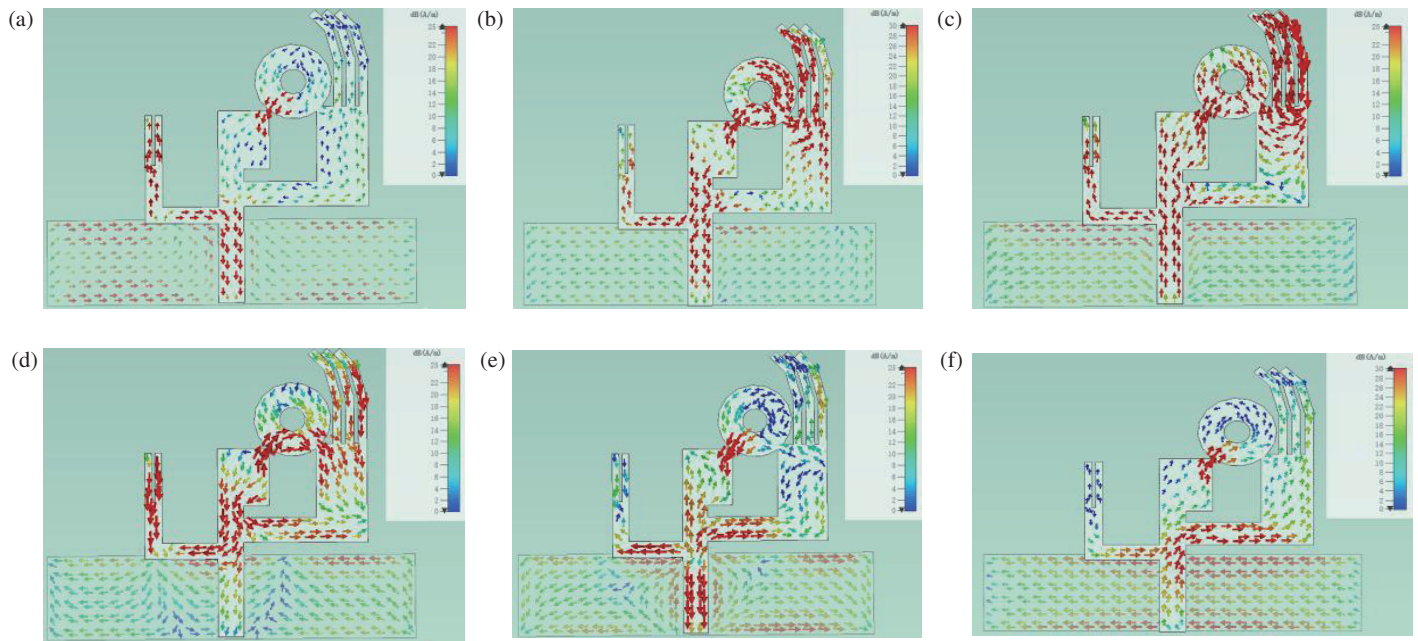


FIGURE 6. Mode current distribution of the improved structure: (a) mode 2 at 5.36 GHz (b) mode 3 at 3.88 GHz (c) mode 5 at 3.32 GHz (d) mode 6 at 6.94 GHz (e) mode 8 at 8.46 GHz (f) mode 9 at 2.48 GHz.

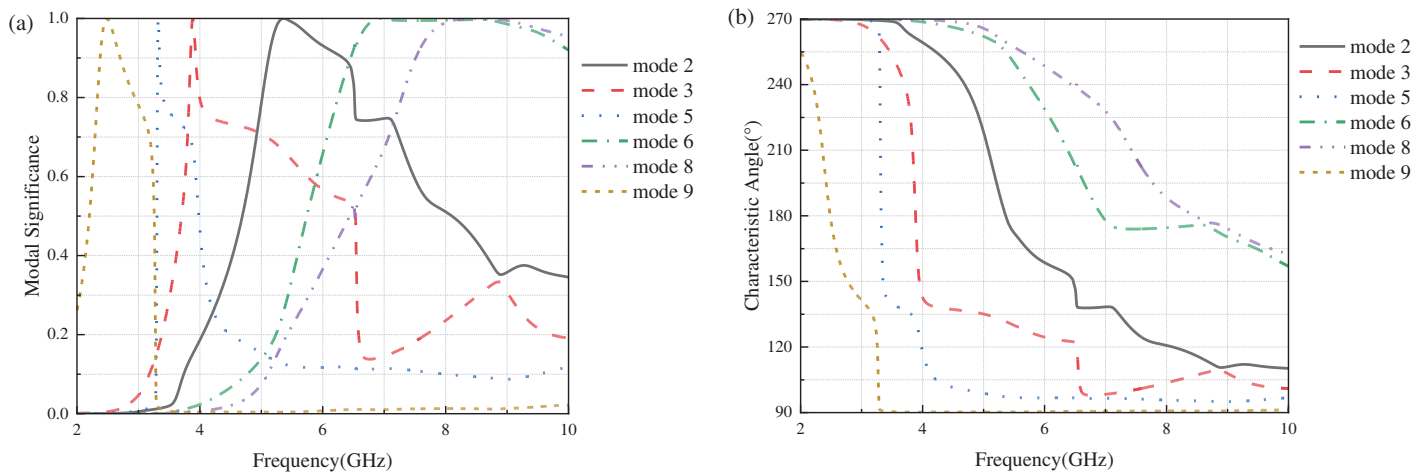


FIGURE 7. The results of mode analysis of the improved structure: (a) MS (b) CA.

trunk to the formed circle. The head of the metal trunk is connected to the formed circle, and a rectangular slot of length xx and width yy is opened above the L-shaped metal on the left side to enhance the current near the feed point.

The S -parameter curve of the improved structure is shown in Figure 3(b). It can be seen that compared with the initial structure, a WiFi band is added, which is 2.33–2.53 GHz. Meanwhile, S_{11} in the 6.18–7.30 GHz band in the initial structure drops below -10 dB, forming a preliminary UWB. In order to expand the frequency band of UWB antenna, the antenna structure needs to be improved again.

The characteristic mode analysis of the improved structure yields the mode current distribution as shown in Figure 6.

The above simulation results show that the currents of mode 2 and mode 8 near the feed point are greatly enhanced

compared to the initial structure, while the currents at the connection between the top of the metal backbone of mode 2 and mode 8 and the circle on the right side are strong, indicating that the formed circle enables mode 2 and mode 8 to be well energized, and the currents at the rectangular slots opened by the L-shaped branches on the left side of mode 6 are enhanced, which is the result of the slots opened at the L-shaped branches.

The MS and CA of the improved structure are shown in Figure 7. As can be seen from Figure 7, the resonance point of mode 3 is shifted forward, which can be well excited and has better excitation effect than the initial structure, and the resonance points of mode 2 and mode 8 are also shifted forward, lowered to 5.36 GHz and 8.46 GHz from 6.5 GHz and 8.8 GHz, respectively, which are more likely to be excited for radiation.

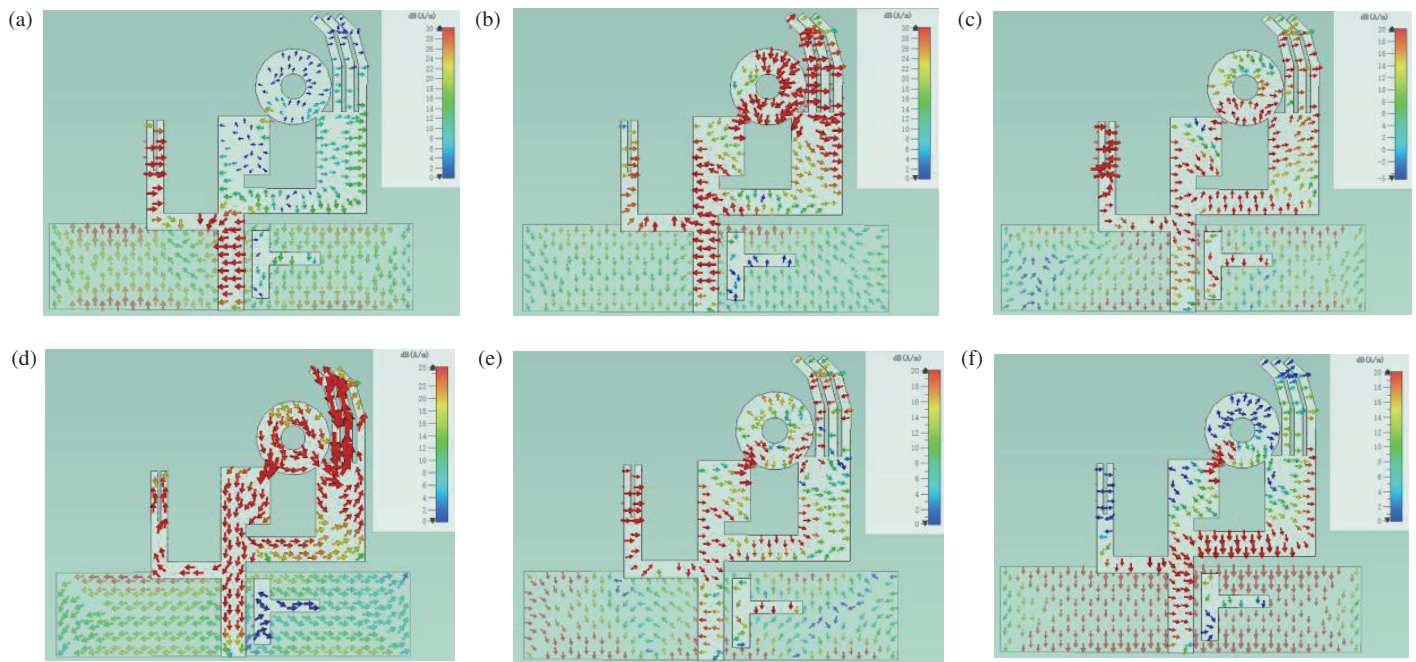


FIGURE 8. Analysis result of the final structure: (a) mode 2 at 5.26 GHz (b) mode 3 at 3.79 GHz (c) mode 5 at 6.54 GHz (d) mode 6 at 9.17 GHz (e) mode 8 at 8.53 GHz (f) mode 9 at 2.45 GHz.

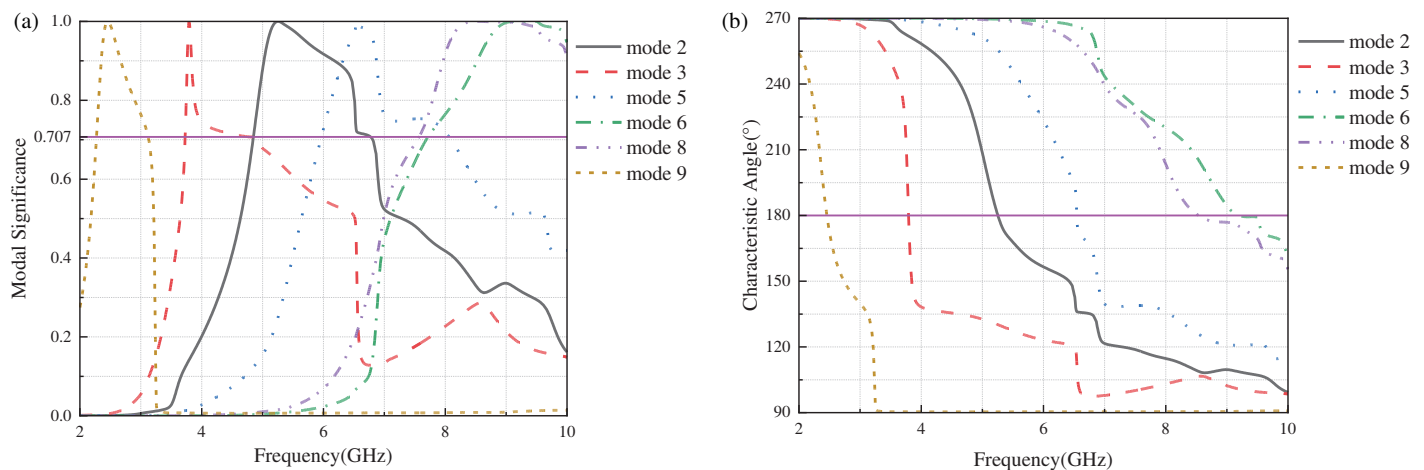


FIGURE 9. The results of mode analysis of the final structure: (a) MS (b) CA.

The resonance point of mode 5 is basically the same as the initial structure. The resonance point of mode 9 has not been changed much, and the resonance point of mode 6 has also been reduced, although it cannot be excited near the feed point. In order to make mode 6 excited again, and at the same time enhance the matching performance to obtain a wider frequency band so that the antenna can better cover the UWB, the antenna structure is improved again by adding a T-shaped metal patch to the right side of the feed line of the metal patch, and the edge of the T-shaped metal is 1.5 mm away from the feed line. The final structure is shown in Figure 2(c).

The S -parameter curve of the final structure is shown in Figure 3(c). Compared with the improved structure, the covered frequency band is wider, ranging from 3.65 to 9.77 GHz,

which meets the requirements of UWB antenna. Meanwhile, S_{11} reaches -43.32 dB at 9.40 GHz, which has a better effect.

The characteristic mode analysis of the final structure is carried out. The simulation results are shown in Figure 8. As can be seen from Figure 8, the analyzed mode currents are very dense at the feed points, indicating that all six analyzed modes are excited, but the excitation structure providing these modes is not the same. According to the current distribution, mode 2 and mode 5 are provided by the left L-shaped branch; mode 3 and mode 6 are provided by the right ring and hand metal; mode 8 is provided by the T-shaped metal patch; and mode 9 is provided by the right metal branch and the connection between the metal trunk and the ring. Multi modes are thus created.

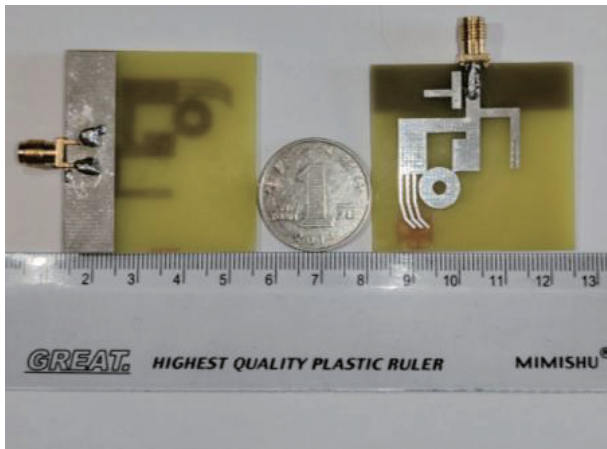


FIGURE 10. The physical model of the proposed antenna.

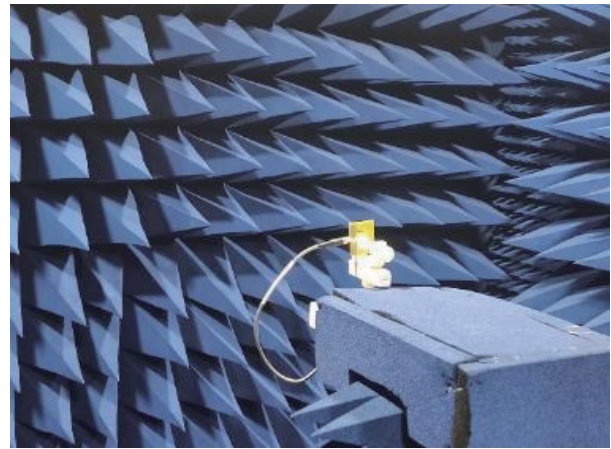


FIGURE 11. The environment of the antenna measurement.

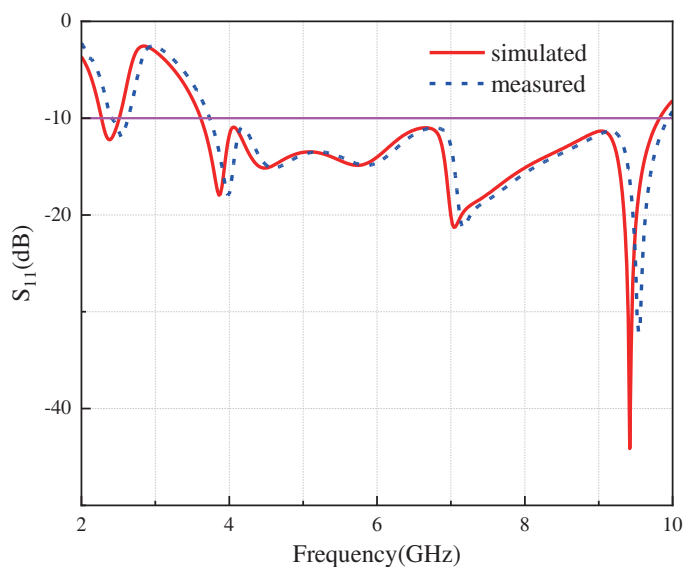


FIGURE 12. Simulated and measured S parameters of the proposed antenna.

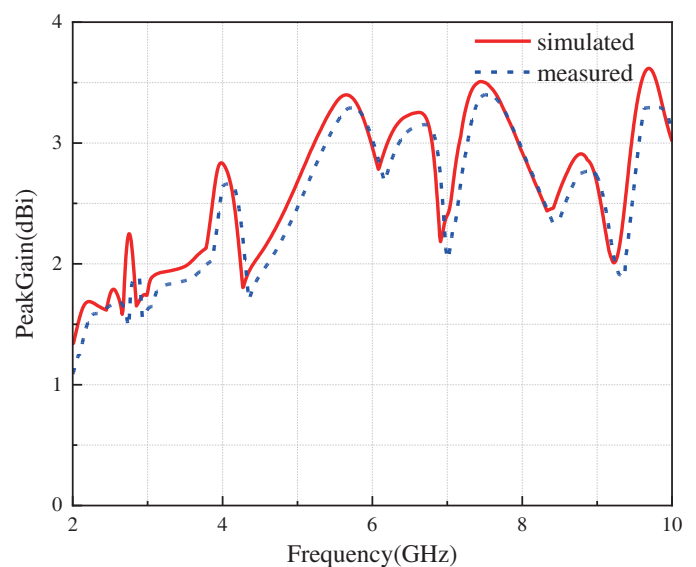


FIGURE 13. Simulated and measured peak gains of the proposed antenna.

According to the above simulation result, the current of mode 6 near the feeding point is greatly enhanced, and the current of the right ring and hand is also enhanced, which indicates that the T-type metal patch makes the matching performance better, thus extending the original frequency band.

The MS and CA of the final structure are shown in Figure 9. It can be seen from Figure 9 that the resonant points of mode 2 and mode 3 move forward, decreasing from 5.36 GHz and 3.88 GHz to 5.26 GHz and 3.79 GHz, respectively, while the resonant points of mode 8 and mode 9 do not change significantly. They act as the radiation mode of the high and low bands, respectively, with the resonant point of mode 6 moving backwards from 6.94 to 9.17 GHz as the radiation mode of the high band together with mode 8, and the resonant point of mode 5 also moving backwards together with mode 2 as the radiation mode of the mid-band. Based on the above analysis results, the six modes described above are all effectively stimulated,

covering the 2.4 GHz band of WiFi and UWB, and meeting the required performance targets.

3. ANTENNA PERFORMANCE

3.1. Antenna Model Measurement

The physical model of the antenna is shown in Figure 10, and the measurement environment is shown in Figure 11. The S -parameters of the antenna are measured by AV3629D vector network analyzer. Figure 12 shows the simulated and measured S -parameter results, which shows good impedance matching within 2.30–2.50 GHz as well as 3.65–9.77 GHz, with relative bandwidths of 4.48% and 91.42%, respectively, and covers the WiFi band and UWB, respectively. At the same time, the measured results are in good agreement with the simulation ones.

At the same time, Figure 13 shows the peak gain of the antenna, and it can be seen that the antenna's gains in the band

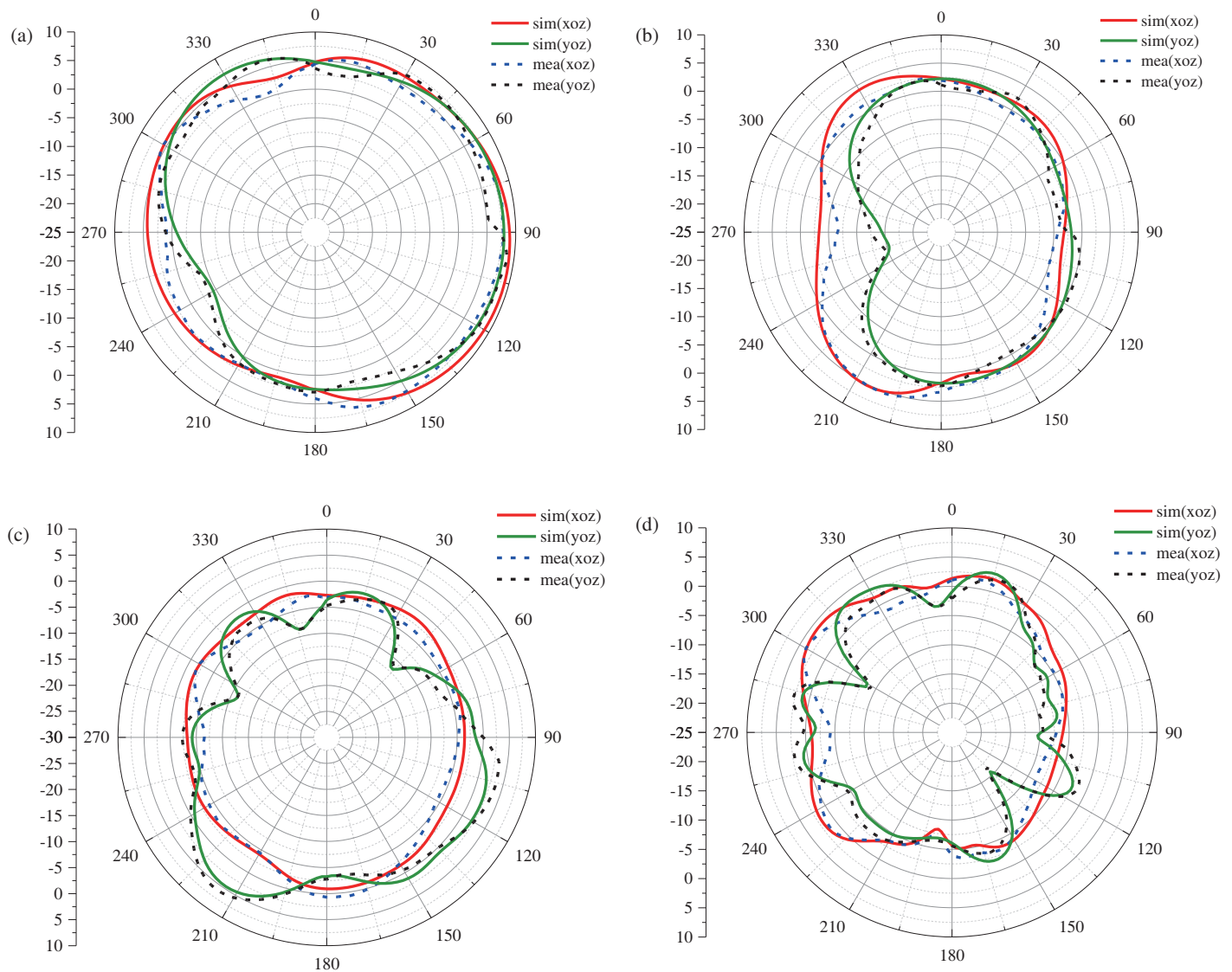


FIGURE 14. Simulated and measured directional patterns: (a) 2.45 GHz (b) 3.85 GHz (c) 7.10 GHz (d) 9.40 GHz.

ranges from 1.35 to 3.62 dBi and at the resonance points are 1.62 dBi, 2.42 dBi, 2.77 dBi, and 2.67 dBi, respectively.

3.2. Orientation Chart

The antenna was tested for its radiation patterns in an anechoic chamber, as shown in Figures 14(a)–(d), which shows the simulated and measured XOZ and YOZ planes of the antenna at 2.45 GHz, 3.85 GHz, 7.10 GHz, and 9.40 GHz.

It can be seen from Figure 14 that the simulation of the four resonance points is basically consistent with the measured direction diagrams of the XOZ and YOZ planes, and the agreement is good. It can be seen from Figure 14(a) that the orientation patterns of XOZ and YOZ planes are approximately a circle and basically exhibit omnidirectional radiation characteristics; in Figure 14(b), XOZ plane is approximately an ellipse, and YOZ plane has better performance in the direction of $0\text{--}270^\circ$. In Figure 14(c), the XOZ plane is approximately a circle, and the YOZ plane is well oriented at $90\text{--}240^\circ$. In Figure

14(d), the XOZ plane is approximately a circle, and the YOZ plane is well directional at $0\text{--}30^\circ$, $105\text{--}125^\circ$, $150\text{--}180^\circ$, $250\text{--}290^\circ$, and $310\text{--}340^\circ$, indicating that energy is concentrated in these parts, showing directional radiation characteristics. It has good performance and can be applied to multi-frequency communication.

3.3. Performance Comparison

To further elaborate the characteristics of the WiFi-UWB antenna proposed in this paper, a comparison of the performance of the antenna designed in this paper with some of the proposed WiFi-UWB antennas is given as shown in Table 2. From Table 2, it can be seen that although the UWB antenna proposed in this paper is not as good as other references in terms of peak gain, it is smaller in size, has a simpler structure, a lower return loss at the resonance point, and certain advantages in terms of band coverage, which is of some value for application in wireless communication networks. Ultra-broadband is charac-

TABLE 2. Antenna performance comparison.

Ref.	Size (mm ³)	Bandwidth (GHz)	S_{11} (dB)	Peak Gain (dBi)
[5]	91.1 × 67.6 × 0.508	2.8–20, 4.4–17.6	–50	10.5
[7]	50 × 55 × 1.6	1.5–3	–48	4.628
[10]	60 × 60 × 1.6	1.75–7.43	–23	16.71
[11]	42 × 25 × 1.6	3.2–12	–28	6.9
[21]	46 × 42 × 1.6	2.12–2.55, 4.67–5.38, 5.7–14.56	–26.51	5.43
[33]	40 × 40 × 1.6	2.8–11.4	–27.5	6
This work	40 × 43 × 1.6	2.30–2.50, 3.65–9.77	–43.32	3.62

terized by high data rate, strong resistance to multipath effect, and low power consumption, which can be applied to a variety of communication fields. In addition, this design covers WiFi bands, including 2.4 GHz band (2.4–2.4835 GHz) and 5 GHz band (5.150–5.350 GHz and 5.725–5.850 GHz), which can realize the omnidirectional radiation, and it can also be applied in 4G/5G communication.

4. CONCLUSION

In this paper, a WiFi-UWB monopole antenna for multi-frequency communication based on characteristic mode theory is designed to cover both the WiFi band and UWB, with an overall return loss of less than –10 dB in the 2.30–2.50 GHz and 3.65–9.77 GHz bands, a gain fluctuating between 1.35 and 3.62 dBi, and a stable directionality in the UWB. The return loss at the resonance frequency of 9.40 GHz reaches –43.32 dB, which has the characteristics of high communication capacity and low-delay wireless communication, and provides the possibility of applications in wireless communication and multi-frequency communication.

ACKNOWLEDGEMENT

This work was supported in part by the Anhui Provincial Natural Science Foundation under Grant No. 2108085MF200, in part by the Natural Science Research Project of Anhui Educational Committee under No. 2022AH051583 and No. 2022AH052138.

REFERENCES

- [1] Lin, X., G. Huang, and Y. Zhang, “An ultra-wideband MIMO antenna based on dual-mode transmission line feeding for wireless communication,” *Progress In Electromagnetics Research M*, Vol. 122, 73–83, 2023.
- [2] Jing, H., G. He, J. Sun, and S. Wang, “Design of a reconfigurable band notch antenna for UWB applications,” *Progress In Electromagnetics Research C*, Vol. 127, 101–112, 2022.
- [3] Panja, A., A. De, B. Roy, P. P. Sarkar, and A. K. Bhattacharjee, “A Letter Box shaped UWB monopole antenna for future 5G communication systems,” in *2023 3rd International conference on Artificial Intelligence and Signal Processing (AISP)*, 1–5, VI-JAYAWADA, India, 2023.
- [4] Xu, R., S. S. Gao, J. Liu, J.-Y. Li, Q. Luo, W. Hu, L. Wen, X.-X. Yang, and J. T. S. Sumantyo, “Analysis and design of ultrawideband circularly polarized antenna and array,” *IEEE Transactions on Antennas and Propagation*, Vol. 68, No. 12, 7842–7853, 2020.
- [5] Liu, J. F., W. Tang, M. Wang, H. C. Zhang, H. F. Ma, X. Fu, and T. J. Cui, “A dual-mode UWB antenna for pattern diversity application,” *IEEE Transactions on Antennas and Propagation*, Vol. 68, No. 4, 3219–3224, 2020.
- [6] Vallappil, A. K., B. A. Khawaja, M. K. A. Rahim, M. N. Iqbal, H. T. Chattha, and M. F. Bin Mohamad Ali, “A compact triple-band UWB inverted triangular antenna with dual-notch band characteristics using SSRR metamaterial structure for use in next-generation wireless systems,” *Fractal and Fractional*, Vol. 6, No. 8, 422, 2022.
- [7] Chauhan, S. and P. K. Singhal, “Design of UWB monopole antenna with EBG structure and ground with rectangular slots,” *International Journal*, Vol. 2, No. 6, 197–201, 2014.
- [8] Nikolaou, S. and M. A. B. Abbasi, “Design and development of a compact UWB monopole antenna with easily-controllable return loss,” *IEEE Transactions on Antennas and Propagation*, Vol. 65, No. 4, 2063–2067, 2017.
- [9] Ibnyaich, S., S. Chabaa, L. Wakrim, A. E. Yassini, A. Zeroual, and M. M. Hassani, “A pentagonal shaped microstrip planar antenna with defected ground structure for ultrawideband applications,” *Wireless Personal Communications*, Vol. 124, 499–515, 2022.
- [10] Kundu, S. and A. Chatterjee, “Sharp triple-notched ultra wideband Antenna with gain augmentation using FSS for ground penetrating radar,” *Wireless Personal Communications*, Vol. 117, No. 2, 1399–1418, 2021.
- [11] Srivastava, G. and A. Mohan, “Compact MIMO slot antenna for UWB applications,” *IEEE Antennas and Wireless Propagation Letters*, Vol. 15, 1057–1060, 2015.
- [12] Awan, W. A., A. Abbas, S. I. Naqvi, D. H. Elkamchouchi, M. Aslam, and N. Hussain, “A conformal tri-band antenna for flexible devices and body-centric wireless communications,” *Micromachines*, Vol. 14, No. 10, 1842, 2023.
- [13] Devarapalli, A. B. and T. Moyra, “CPW-fed dual-element metamaterial inspired multiband antenna using simple FSS for gain enhancement,” *Optik*, Vol. 290, 171313, 2023.
- [14] Kumar, A., P. Pattanayak, R. K. Verma, D. Sabat, and G. Prasad, “Two-element MIMO antenna system for multiband millimeter-wave, 5G mobile communication, Ka-band, and future 6G applications with SAR analysis,” *AEU — International Journal of Electronics and Communications*, Vol. 171, 154876, 2023.

- [15] Mangal, J. and N. Gupta, "An Annular switchable antenna for WiFi, WiMax, WLAN & UWB frequency range applications," in *2021 International Conference on Control, Automation, Power and Signal Processing (CAPS)*, 1–4, Jabalpur, India, 2021.
- [16] Noghianian, S., "Dual-band wearable MIMO antenna for WiFi sensing applications," *Sensors*, Vol. 22, No. 23, 9257, 2022.
- [17] Wang, D. and C. H. Chan, "Multiband antenna for WiFi and WiGig communications," *IEEE Antennas and Wireless Propagation Letters*, Vol. 15, 309–312, 2015.
- [18] Tsai, C.-J. and B.-Y. Tsai, "A U-matched printed antenna for dual-band WiFi applications," *International Journal of Microwave and Wireless Technologies*, Vol. 7, No. 5, 551–556, 2015.
- [19] Khurshid, A., J. Dong, and R. Shi, "A metamaterial-based compact planar monopole antenna for Wi-Fi and UWB applications," *Sensors*, Vol. 19, No. 24, 5426, 2019.
- [20] Djellid, A., F. Benmeddour, L. Bahri, and A. Ghodbane, "Novel high-gain and compact UWB microstrip antenna for WiFi, WiMAX, WLAN, X band and 5G applications," *Optical and Quantum Electronics*, Vol. 54, No. 7, 441, 2022.
- [21] Wang, Z., M. Wang, and W. Nie, "A monopole UWB antenna for WiFi 7/Bluetooth and satellite communication," *Symmetry*, Vol. 14, No. 9, 1929, 2022.
- [22] Mangal, J. and L. A. Varma, "A miniaturized trapped slotted triangular mounted patch antenna for GPS, WiMax, WBAN, WiFi, and UWB frequency range applications," in *2022 2nd Odisha International Conference on Electrical Power Engineering, Communication and Computing Technology (ODICON)*, 1–5, Bhubaneswar, India, 2022.
- [23] Nihade, T., Z. Alia, A. T. Naima, and R. Faouzi, "A novel compact UWB monopole antenna with reconfigurable dual band-notch characteristics for wimax and wifi 6e bands," in *2020 International Symposium on Advanced Electrical and Communication Technologies (ISAECT)*, 1–5, Marrakech, Morocco, 2020.
- [24] Jabire, A. H., A. Ghaffar, X. J. Li, A. Abdu, S. Saminu, M. Alibakhshikenari, F. Falcone, and E. Limiti, "Metamaterial based design of compact UWB/MIMO monopoles antenna with characteristic mode analysis," *Applied Sciences*, Vol. 11, No. 4, 1542, 2021.
- [25] Abdul-Rahman, E. and D. N. Aloï, "Design of a 5G sub-6 GHz vehicular cellular antenna element with consistent radiation pattern using characteristic mode analysis," *Sensors*, Vol. 22, No. 22, 8862, 2022.
- [26] Peñafiel-Ojeda, C. R., C. E. Andrade, R. Baez-Egas, and V. Garcia-Santos, "An ultrawideband printed monopole antenna analyzed with the theory of characteristic modes," *IEEE Latin America Transactions*, Vol. 20, No. 6, 948–954, 2022.
- [27] Singh, H. V. and S. Tripathi, "Compact UWB MIMO antenna with cross-shaped unconnected ground stub using characteristic mode analysis," *Microwave and Optical Technology Letters*, Vol. 61, No. 7, 1874–1881, 2019.
- [28] Wu, W. and Y. P. Zhang, "Analysis of ultra-wideband printed planar quasi-monopole antennas using the theory of characteristic modes," *IEEE Antennas and Propagation Magazine*, Vol. 52, No. 6, 67–77, 2010.
- [29] Mohanty, A., B. R. Behera, and N. Nasimuddin, "Reconfigurable miniaturized UWB multiple-input-multiple-output antenna system design and study using characteristics mode analysis," *International Journal of RF and Microwave Computer-Aided Engineering*, Vol. 32, No. 9, e23287, 2022.
- [30] Ghanbari, L., A. Keshtkar, and S. Jarchi, "A novel metamaterial-inspired UWB and ISM multiband antenna for wireless communications: Design and characteristic mode analysis," *Progress In Electromagnetics Research C*, Vol. 136, 1–12, 2023.
- [31] Mohanty, A. and B. R. Behera, "Investigation of 2-port UWB MIMO diversity antenna design using characteristics mode analysis," *AEU — International Journal of Electronics and Communications*, Vol. 124, 153361, 2020.
- [32] Suresh, A. C., T. S. Reddy, B. T. P. Madhav, S. Alshathri, W. El-Shafai, S. Das, and V. Sorathiya, "A novel design of spike-shaped miniaturized 4×4 MIMO antenna for wireless UWB network applications using characteristic mode analysis," *Micro-machines*, Vol. 14, No. 3, 612, 2023.
- [33] Suresh, A. C. and T. Reddy, "Experimental investigation of novel frock-shaped miniaturized 4×4 UWB MIMO antenna using characteristic mode analysis," *Progress In Electromagnetics Research B*, Vol. 101, 45–61, 2023.
- [34] Zhang, Q., R. Ma, W. Su, and Y. Gao, "Design of a multimode UWB antenna using characteristic mode analysis," *IEEE Transactions on Antennas and Propagation*, Vol. 66, No. 7, 3712–3717, 2018.